

Near-Visible Light Generation of a Quinone Methide from 3-Hydroxymethyl-2-anthrol

Dani Škalamera,[†] Kata Mlinarić-Majerski,[†] Irena Martin-Kleiner,[‡] Marijeta Kralj,[‡] Peter Wan,[§] and Nikola Basarić^{*,†}

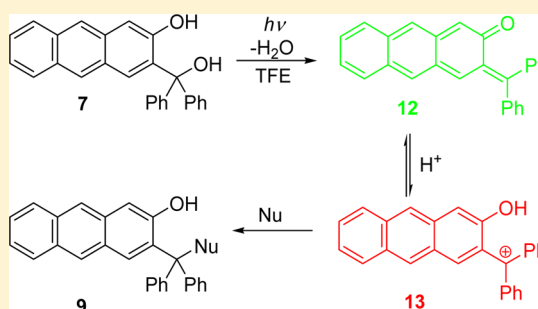
[†]Department of Organic Chemistry and Biochemistry, Ruđer Bošković Institute, Bijenička cesta 54, 10 000 Zagreb, Croatia

[‡]Department of Molecular Medicine, Ruđer Bošković Institute, Bijenička cesta 54, 10 000 Zagreb, Croatia

[§]Department of Chemistry, University of Victoria, Box 3065 Stn CSC, Victoria BC V8W 3V6, Canada

Supporting Information

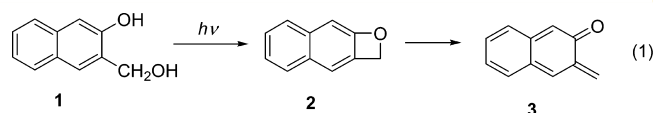
ABSTRACT: Excitation of 2-hydroxy-3-(diphenylhydroxymethyl)-anthracene (**7**) to S_1 initiates photodehydration, giving the corresponding quinone methide (QM) that was detected by laser flash photolysis (LFP) in 2,2,2-trifluoroethanol ($\lambda = 580$ nm, $\tau = 690 \pm 10$ ns). The QM decays by protonation, giving a cation ($\lambda = 520$ nm, $\tau = 84 \pm 3$ μ s), which subsequently reacts with nucleophiles. The rate constants in the reactions with nucleophiles were determined by LFP, whereas the adducts were isolated via preparative photolyses. The photogeneration of QMs in the anthrol series is important for potential use in biological systems since the chromophore absorbs at wavelengths > 400 nm. Antiproliferative investigations conducted with 2-anthrol derivative **7** on three human cancer cell lines showed higher activity for irradiated cells.



INTRODUCTION

Quinone methides (QMs) are common reactive intermediates in chemistry and in the photochemistry of phenols, attracting much attention recently owing to their biological activity.¹ Although the partial zwitterionic character of QMs makes them both electrophilic and nucleophilic, their reactivity with nucleophiles is especially important in biological systems. It has been demonstrated that QMs react with amino acids² and proteins³ and inhibit the action of some enzymes.⁴ Moreover, QMs also react with nucleotides,⁵ inducing alkylation and the cross-linking of DNA.⁶ The ability of QMs to cross-link DNA renders them as potential anticancer therapeutics.⁷ Some antineoplastic agents such as mitomycin⁸ base their antiproliferative action on the metabolic formation of QMs that alkylate DNA. Moreover, some classes of anthracyclines such as daunomycin, which base their action on DNA cross-linking, also metabolically form QMs.⁹ However, later, it was shown that QMs are not responsible reagents that cross-link DNA, but it probably involves metabolic formation of formaldehyde.¹⁰

QMs can be formed under mild conditions in photochemical reactions of suitably substituted phenols, such as photodehydroxylation of hydroxybenzylphenols,¹¹ and photoelimination of acetic acid,¹² amines,¹³ or ammonium salts.^{2b} Photodehydration has also been reported in the larger chromophoric systems, such as suitably substituted phenylphenols¹⁴ and naphthols.¹⁵ Popik et al. studied photodehydration of naphthol **1**, which gave benzoxete intermediate **2** that subsequently underwent ring-opening to QM **3** (eq 1).¹⁶ The photogeneration of naphthalene QMs was later applied to photocaging¹⁷ and for surface modification and photolithography.¹⁸



We became interested in the photochemical formation of sterically congested QMs that have potential biological applicability.¹⁹ Photocytotoxicity was investigated on three human cancer lines. Photoinduced antiproliferative activity was also reported for naphthol,^{15b} 1,1'-bi-2-naphthol (BINOL),²⁰ and naphthalene diimide QM derivatives.²¹ For ultimate application *in vivo*, it is essential to develop systems that can photogenerate QMs when excited with light of longer wavelengths (>350 nm). However, the photogeneration of QMs by photodehydration reaction in 2-anthrols or larger chromophoric systems has never been reported. Herein, we report the first example of photochemical QM formation (via dehydration) in an anthrol derivative **7**. The photoreactivity was studied by preparative irradiations, fluorescence measurements, and by laser flash photolysis (LFP). Antiproliferative investigation was performed on three human cancer cell lines with and without irradiation.

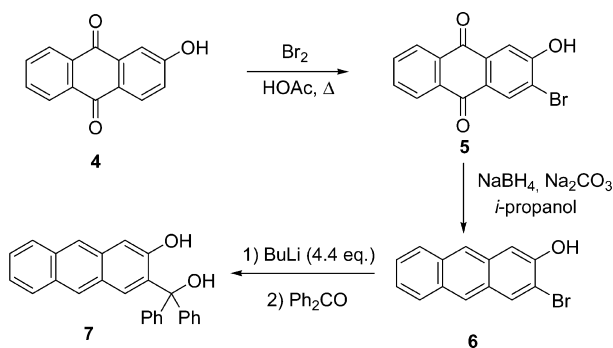
RESULTS AND DISCUSSION

Synthesis of the new anthrol **7** was accomplished in 4 steps, starting from the commercially available 2-aminoanthraquinone, which was converted to 2-hydroxyanthraquinone (**4**) via a known procedure.²² Bromination of **4** afforded 3-bromo

Received: February 6, 2014

Published: April 23, 2014

Scheme 1



derivative **5** (40%), and 1,3-dibromo derivative (38%), which was separated from **5** by a column chromatography (Scheme 1). Subsequent reduction of **5** gave 2-bromo-3-anthrol (**6**) in 80% yield and a small amount of 2-anthrol (**8**) due to undesired concomitant debromination. Lithiation with an excess of BuLi and quenching with benzophenone furnished **7** in 40% yield.

Absorption spectra of **7** and **8** in CH₃CN solution exhibit an absorption band of lowest energy centered between 350 and 400 nm, 50 nm bathochromically shifted compared to that of anthracene. The pK_a of 2-anthrol (**8**) in CH₃CN–H₂O (1:9) in S₀ and S₁ was determined by UV–vis and fluorescence titration, respectively (pK_a = 9.40 ± 0.03; pK_a^{*} = 2.13 ± 0.01; see the Supporting Information). Since it is known that intramolecular H-bonding with the benzyl alcohol increases acidity in 2-naphthol,¹⁶ the anticipated pK_a values for **7** are expected to be somewhat lower.

The photophysical properties of **7** and **8** were investigated in CH₃CN and CH₃CN–H₂O (1:1). Results are compiled in Table 1. Fluorescence in aqueous solution is quenched

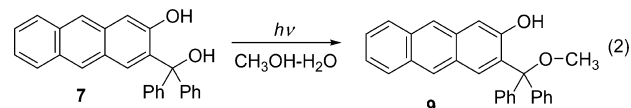
Table 1. Photophysical Properties of 7 and 8 in CH₃CN and CH₃CN–H₂O (1:1)

	7	8
Φ _F (CH ₃ CN) ^a	0.86 ± 0.01	0.88 ± 0.05
Φ _F (CH ₃ CN–H ₂ O) ^a	0.39 ± 0.01	0.57 ± 0.02
τ (CH ₃ CN)/ns ^b	17.8 ± 0.1	25.3 ± 0.1
τ (CH ₃ CN–H ₂ O)/ns ^b	1.7 ± 0.2 phenolate 8.1 ± 0.2 phenolate 24.5 ± 0.1 phenol	15.4 ± 0.1 phenolate 25.3 ± 0.1 phenol

^aQuantum yields of fluorescence measured by use of quinine sulfate in 0.05 M aqueous H₂SO₄ (Φ_F = 0.53) as a reference.²⁴ ^bFluorescence lifetimes measured by time-correlated single-photon timing method.

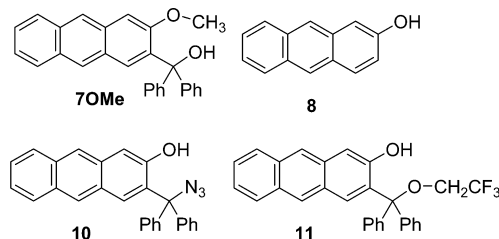
compared to that in neat CH₃CN. The quenching is due to proton transfer (PT) to solvent. Furthermore, the Φ_F for **7** in both solvents is lower than that for **8**. Since **8** cannot give QMs, the lower Φ_F of **7** may be due to the photochemical pathway giving QM. Contrary to 2-methoxyanthracene,²³ **7** and **8** are characterized by a single exponential decay of fluorescence in CH₃CN. Addition of H₂O changes the decay. For **8**, it becomes double-exponential with a rise component (assigned to phenolate) that contributes more at longer wavelengths. For **7**, the best fit was obtained by a three-exponential function with two rise components. Although a firm elucidation of the decay kinetics cannot be made at this time, the finding is consistent with a scheme that photodissociation of the anthrol OH of **7** in S₁ triggers elimination of OH[−] (overall loss of H₂O) that leads to the formation of QM.

Photochemical solvolysis of **7** was investigated by irradiations in CH₃OH–H₂O (see the Supporting Information). Irradiations gave cleanly one product (**9**, eq 2). Conversion to **9** after



1 h of irradiation was higher in the presence of 20% H₂O (≈70%) than in neat CH₃OH (≈50%). Such a finding has been reported in systems wherein the phenolic OH is not H-bonded to the benzylic alcohol¹⁹ and explained by a higher ability of phenols to deprotonate in S₁ to clusters of H₂O than CH₃OH.²⁵

Photosolvolysis of trityl derivatives can, in principle, take place via carbocations. To probe if **7** undergoes heterolytic cleavage of OH to give carbocation **13** (Scheme 2), irradiation of **7OMe** was performed. However, in the condition where **7** gave 72% of **9**, **7OMe** remained unchanged. This finding indicates that the free phenolic OH is required for the formation of the solvolysis product. Furthermore, the finding is in accord with the photosolvolysis mechanism involving QM **12** (*vide infra*).



The scope of the photosolvolysis was further investigated by performing irradiations in the presence of other nucleophiles. Thus, azide adduct **10** and 2,2,2-trifluoroethanol (TFE) adduct **11** were isolated after irradiation of **7** in CH₃CN–H₂O and CH₃CN–TFE, respectively, in ≈35–40% yield. The structures of the photoproducts **9**, **10**, and **11** were confirmed by NMR analysis. Additionally, all photosolvolyses were achieved by use of light > 350 nm (350 nm, 420 nm, and vis-lamps; see the Supporting Information).

The efficiency of the photosolvolysis in CH₃OH–H₂O (4:1) was determined by simultaneous use of three actinometers, valerophenone, KI/KIO₃, and ferrioxalate.²⁶ Irradiation was performed by use of monochromatic light at 254 nm, and the composition of the irradiated solution of **7** was analyzed by HPLC. All actinometers gave Φ_R = 0.023 ± 0.001 for reaction.

To probe for QM and other plausible long-lived intermediates in the photochemistry of **7**, LFP measurements were performed. The samples were excited by use of a Nd:YAG laser at 354 nm. The measurements were performed in CH₃CN and CH₃CN–H₂O (1:1), and the difference was anticipated due to PT in the aqueous solution. In CH₃CN solution (N₂- and O₂-purged), a band centered at 700 nm can be seen (τ = 1.0 ± 0.1 μs) that, in the aqueous solution, decays during the laser pulse. The transient is tentatively assigned to the anthrol radical cation, which, in the aqueous solution, decays by deprotonation.²⁷ In addition, in both solvents, more persistent transients were detected absorbing at shorter wavelengths of 400–600 nm. The decay is multiexponential, revealing several species. The major contribution to the band more centered at shorter wavelengths (400–500 nm) decays slower (τ ≈ 10–100 μs and τ ≈ 0.1–2 s) and can also be seen in the transient spectra of **8** (see the

Scheme 2

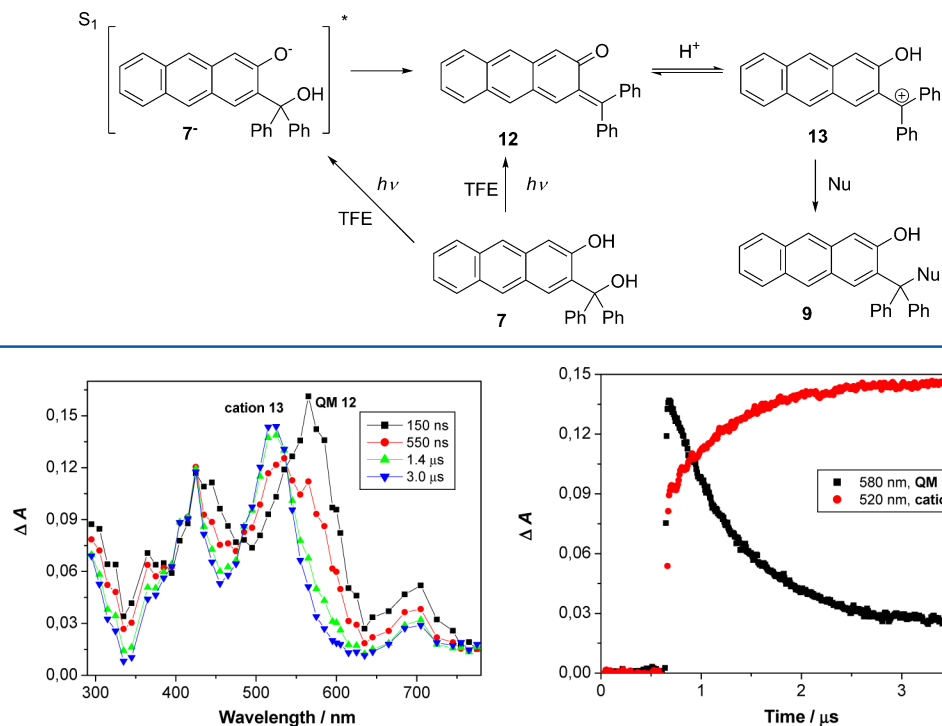


Figure 1. Transient absorption spectra of **7** in O_2 -purged 2,2,2-trifluoroethanol (TFE) (left), and growth and decay of the transient absorption at 520 nm (corresponding to cation **13**) and 580 nm (corresponding to QM **12**), respectively (right).

Supporting Information). The transients are not affected by the presence of O_2 and H_2O . The shorter-lived species is tentatively assigned to phenoxyl radical, according to the comparison with the published spectra and decay kinetics.²⁸ In addition, a transient absorption was detected at 500–600 nm that decays multi-exponentially that could be quenched by nucleophiles (and not by O_2). Therefore, this transient could tentatively be assigned to QMs or other electrophilic species (see the Supporting Information). However, because of complex decay kinetics and overlapping of the transient absorption spectra with several other species, no firm assignment to a QM can be made at this time.

A cleaner picture was obtained for LFP experiments carried out in TFE. TFE is a polar non-nucleophilic solvent in which electrophilic species such as QMs^{14,15,19} and carbocations²⁹ exhibit longer lifetimes. LFP measurement for **7** in O_2 -purged TFE gave rise to a strong transient absorption centered at 580 nm that is formed within the laser pulse. It decayed ($k_{12 \rightarrow 13} = 1.4 \times 10^6 \text{ s}^{-1}$, $\tau = 690 \pm 10 \text{ ns}$), giving a new species absorbing at 520 nm (Figure 1) that also decays ($k_{13 \rightarrow 9} = 1.4 \times 10^4 \text{ s}^{-1}$, $\tau = 84 \pm 3 \mu\text{s}$). Addition of ethanolamine, a ubiquitous quencher of QMs,^{14,19} changed the appearance of the spectra. However, the decay of the absorption at 580 nm was slower, and faster at 520 nm, giving one band in the spectra. This finding suggests that two species are in equilibrium that is influenced by pH (ethanolamine is a base). Quenching with nucleophiles was successful for species absorbing at 520 nm (not affecting the faster decay at 580 nm). The quenching rate constants are compiled in Table 2. According to the quenching data and the position of the maximum in the absorption spectra (comparison with the known spectra of trityl cation),³⁰ the long-lived transient was assigned to carbocation **13**. Since the short-lived transient is sensitive to acidity and in equilibrium with the cation, it is tentatively assigned to QM **12**. Consequently, the

Table 2. Rate Constants for the Quenching of Cation **13** with Nucleophiles (k_q or $k_{13 \rightarrow 9}/\text{s}^{-1} \text{ M}^{-1}$)^a

nucleophile	$k_q/\text{s}^{-1} \text{ M}^{-1}$
CH_3OH	9.8×10^3
H_2O	1.6×10^3
NaN_3	2.1×10^8

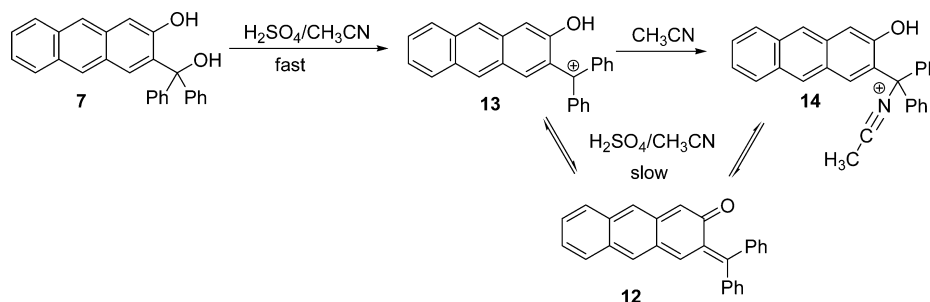
^aMeasurements performed in air-saturated TFE.

first detected species in TFE by LFP is QM **12**, which decays by protonation, giving cation **13** (Scheme 2). Subsequent reaction with nucleophiles furnishes adducts. Interestingly, ethanolamine did not quench QM **12** in the tested concentration. The finding was explained by the ethanolamine basicity ($\text{p}K_a = 9.5$), which prevented fast protonation of QM **12** to cation **13**.

Cation **13** can also be formed in the CH_3CN solution in a thermal acid-catalyzed reaction and detected by UV-vis spectroscopy. To the CH_3CN solution was added H_2SO_4 ($c = 0.25 \text{ M}$), resulting in an immediate color change to red. The difference absorption spectrum has a maximum at 520 nm (see the Supporting Information) with another band at longer wavelengths ($\approx 700 \text{ nm}$) and resembles the transient absorption of **7** measured in TFE and 1,1,1,3,3,3-hexafluoroisopropanol (HFIP) after decay of the short-lived species assigned to QM **12**. The transient in CH_3CN decays ($\tau = 0.63 \pm 0.02 \text{ min}$), probably giving CH_3CN adduct **14**, resulting in a colorless solution. However, within 45–60 min, a new species is formed absorbing at 500–700 nm, resulting in a green color. The latter is tentatively assigned to QM **12** formed in a thermal acid-catalyzed reaction (Scheme 3).

Antiproliferative investigation was conducted with **7** on three human cancer cell lines, HCT 116 (colon), MCF-7 (breast), and H 460 (lung), with and without exposure to irradiation

Scheme 3



(350 and 420 nm). In addition, the cells were irradiated in the absence of compounds to check for the cytotoxic effect of irradiations. The results are compiled in Table 3. Irradiation of

Table 3. IC₅₀ Values (in μM) for **7**^a

cell lines	HCT 116	MCF-7	H 460
not irradiated	21 ± 0.3	20 ± 0.5	19 ± 1
3 × 5 min 350 nm	2 ± 0.4	4 ± 3	3 ± 1
3 × 5 min 420 nm	2 ± 0.4	2 ± 0.1	2 ± 0.2

^aIC₅₀: the concentration that causes 50% growth inhibition. Irradiation of the cells at 350 nm that were not treated with **7** induced up to a maximum 25% inhibition of tumor cell growth, whereas irradiation of untreated cells at 420 nm showed no effect. For the calculation of IC₅₀, see the Experimental Section.

the cells at 350 nm that were not treated with **7** induced up to a maximum 25% of inhibition of tumor cell growth, whereas 420 nm did not cause any significant inhibition of tumor cell growth. On the other hand, exposure of the cells treated with **7** to irradiation induced a higher cytotoxic effect than cells that were kept in the dark. Consequently, higher photocytotoxicity of the compound allows for potential biological applications. However, for the actual photochemotherapeutic applications (except for maybe some forms of skin cancer), the compounds should bear chromophores absorbing at >600 nm. Photochemically induced higher cytotoxicity of **7** suggests that the enhanced antiproliferative activity is due to the photo-generation of QMs. Although the exact mechanism of the enhanced antiproliferative activity was not determined, it is presumed that it is due to the reactivity of **12** or **13** with DNA,^{5,6} as well as some particular proteins (e.g., enzymes).^{2–4} Since the LFP experiments did not indicate formation of the triplet excited state, singlet oxygen probably did not induce antiproliferative activity. The investigation of biological action of different anthrol derivatives is currently under way and will be published separately.

CONCLUSION

The presented results show that dehydration of 2-anthrol derivative **7** to QM **12** can be initiated in a photochemical reaction and probably involves deprotonation of the phenol OH as the first step, followed by expulsion of the alcohol OH⁻. However, we could not time-resolve the formation of QM **12** (it is formed within the laser pulse). Therefore, we cannot rule out mechanisms that involve (i) excited-state intramolecular proton transfer (ESIPT) from the phenol OH to the benzyl alcohol that is coupled with dehydration or (ii) formation of a benzoxete intermediate that has a lifetime of <50 ns and subsequently ring-opens to form the QM.

Photogeneration of QMs in the anthrol series that can be initiated by near-visible light is of particular importance in biological systems. Preliminary results of antiproliferative investigations conducted for **7** on three human cancer cell lines showed higher activity for the cells that were irradiated. Consequently, we believe that anthrol derivatives have potential as a new class of photochemotherapeutic reagents, or as photolabeling markers for biological systems.

EXPERIMENTAL SECTION

Experimental Procedure, General. ¹H and ¹³C NMR spectra were recorded at 300 or 600 MHz at rt using TMS as a reference, and chemical shifts were reported in parts per million (ppm). Melting points were determined using a Mikroheiztisch apparatus and were not corrected. IR spectra were recorded on a spectrophotometer in KBr, and the characteristic peak values were given in cm⁻¹. HRMS were obtained on a MALDI TOF/TOF instrument. For the sample analysis, an HPLC was used with a C18 (1.8 μm, 4.6 × 50 mm) column. HPLC runs were conducted at rt (~25 °C), and chromatograms were recorded using a UV detector at 254 nm. Other HPLC data are given in the Supporting Information, since the parameters vary. For the chromatographic separations, silica gel (0.05–0.2 mm) was used. Irradiation experiments were performed in a reactor equipped with 16 lamps with the output at 350 nm or a reactor equipped with 8 lamps. During the irradiations, the irradiated solutions were continuously purged with Ar and cooled by a tap water finger condenser. Solvents for irradiations were of HPLC purity. Chemicals were purchased from the usual commercial sources and were used as received. 2-Hydroxyanthraquinone (**4**) was prepared from commercially available 2-aminoanthraquinone according to the known procedure.²² Solvents for chromatographic separations were used as they are delivered from the supplier (p.a. grade) or purified by distillation (CH₂Cl₂). Diethyl ether used for the reaction with BuLi was previously refluxed over Na and freshly distilled.

3-Bromo-2-hydroxyanthraquinone (5). The reaction was carried out in a two-neck round-bottom flask (250 mL) equipped with a condenser and a dropping funnel. 2-Hydroxyanthraquinone (**4**, 4.54 g, 20.2 mmol) was dissolved in glacial acetic acid (50 mL) by heating using an oil bath. Bromine (5 mL, 97.2 mmol) in glacial acetic acid (50 mL) was added to the refluxing reaction mixture over 4 h, and the refluxing was continued overnight (16 h). The progress of the reaction was monitored by HPLC (see the Supporting Information). The next day, the reaction mixture was allowed to cool to rt and poured on water (300 mL). A saturated solution of Na₂SO₃ was added to destroy the excess of bromine. The yellow precipitate was filtered off, washed with water until neutral (tested with universal indicator paper), and dried in a desiccator over KOH overnight. The crude product contained 3-bromo-2-hydroxyanthraquinone (**5**) and 1,3-dibromohydroxyanthraquinone in a 1:1 ratio. These two compounds were separated using column chromatography (SiO₂, CH₂Cl₂/EtOAc/HOAc 760:40:1 to 720:80:1) to obtain 1,3-dibromo-2-hydroxyanthraquinone **5** (2.93 g, 7.68 mmol, 38% yield) and 3-bromo-2-hydroxyanthraquinone (2.45 g, 8.08 mmol, 40% yield) as yellow solid substances.

1,3-Dibromo-2-hydroxyanthraquinone. ^1H NMR (300 MHz, $\text{DMSO}-d_6$) δ /ppm 8.34 (s, 1H), 8.18–8.10 (m, 2H), 7.93–7.87 (m, 2H); IR (KBr) $\nu_{\text{max}}/\text{cm}^{-1}$ 3412 (O-H), 3105 (C-H), 3070 (C-H), 1672 (C=O).

3-Bromo-2-hydroxyanthraquinone (5).³¹ Yellow solid, mp 235–245 °C; ^1H NMR (300 MHz, $\text{DMSO}-d_6$) δ /ppm 11.97 (s, 1H), 8.22 (s, 1H), 8.17–8.11 (m, 2H), 7.95–7.86 (m, 2H), 7.64 (s, 1H); ^{13}C NMR (150 MHz, $\text{DMSO}-d_6$) δ /ppm 182.0 (s), 180.3 (s), 159.6 (s), 134.5 (d), 134.2 (d), 134.0 (s), 132.9 (s), 132.8 (s), 132.1 (d), 126.6 (d, 2C), 125.8 (s), 116.6 (s), 112.8 (d); IR (KBr) $\nu_{\text{max}}/\text{cm}^{-1}$ 3350 (O-H), 1668 (C=O), 1570 (C=O), 1274 (C-H), 719 (C-H); HRMS (MALDI) calculated for $\text{C}_{14}\text{H}_7\text{BrK}_3^+$ 340.9210, found 340.9204.

3-Bromo-2-hydroxyanthracene (6). NaBH_4 (454 mg, 12 mmol) was dissolved in 1 M Na_2CO_3 (aq) (30 mL), *i*-propanol (5 mL) was added (foaming suppressor), and the mixture was heated until the boiling point was achieved. 3-Bromo-2-hydroxyanthraquinone (5, 910 mg, 3 mmol) was added in three portions. The reaction mixture was refluxed for 15 min (longer reflux time usually produced more debromination product, 2-hydroxyanthracene). The reaction was quenched by careful addition of ice-cooled water (30 mL), followed by the addition of 3 M HCl until acidic reaction was achieved (tested by universal indicator paper). The product was collected by filtration, washed with water (until neutral reaction of the filtrate was achieved), and dried in an evacuated desiccator (10 mbar) over KOH overnight. The crude product was purified on a column of silica gel using dichloromethane as eluent to give pure product 6 (656 mg, 2.4 mmol, 80% yield over two steps) as a yellow powder: mp 225–232 °C; ^1H NMR (300 MHz, CDCl_3) δ /ppm 8.27 (s, 1H), 8.24 (s, 1H), 8.22 (s, 1H), 7.93 (t, $J = 7.2$ Hz, 2H), 7.50 (s, 1H), 7.48–7.38 (m, 2H), 5.64 (s, 1H); ^{13}C NMR (300 MHz, $\text{DMSO}-d_6$) δ /ppm 150.9 (s), 132.0 (d), 131.7 (s), 131.5 (s), 129.7 (s), 128.0 (d), 127.7 (s), 127.4 (d), 125.7 (d), 125.1 (d), 124.6 (d), 123.1 (d), 114.7 (s), 107.8 (d); IR (KBr) $\nu_{\text{max}}/\text{cm}^{-1}$ 3512 (O-H), 3049 (C-H); HRMS (MALDI) calculated for $\text{C}_{14}\text{H}_9\text{BrO}^+$ 271.9831, found 271.9829.

2-Hydroxy-3-(diphenylhydroxymethyl)anthracene (7). The reaction was carried out in a two-neck round-bottom flask (50 mL) under a N_2 inert atmosphere, equipped with a N_2 balloon and a septum. The flask was charged with 3-bromo-2-hydroxyanthracene (6, 286 mg, 1.00 mmol) and dry Et_2O (10 mL) and cooled in an ice-methanol bath (–15 to –10 °C). BuLi (2.5 M in hexanes, 1.2 mL, 3.00 mmol) was added dropwise over 15 min, changing the color to brown. The reaction mixture was then emerged from the ice bath and stirred for 15 min at rt, whereby all the solid compound was dissolved, giving a clear brown solution. The reaction mixture was then again cooled to –10 °C, and benzophenone (900 mg, 4.94 mmol) in dry Et_2O (4 mL) was added. Stirring was continued 1 h at –10 °C. Then, the reaction mixture was allowed to reach rt, and the stirring was continued overnight. The reaction was quenched by careful addition of water (15 mL) and transferred to the separation funnel. A solution of 1 M NaOH (20 mL) and water (100 mL) was added, and the aqueous layer was extracted with hexane (2 × 20 mL) in order to remove unreacted benzophenone and the product of the reaction of benzophenone with BuLi . The aqueous layer was then acidified with 10% acetic acid and extracted with Et_2O (3 × 25 mL). The ether extracts were combined and dried over anhydrous MgSO_4 . After filtration and removal of the solvent, the crude product was purified on a column of silica gel using dichloromethane as eluent to give pure 7 (763 mg, 2.03 mmol, 40% yield) in the form of a yellow-orange solid. mp 199–200 °C; ^1H NMR (300 MHz, $\text{DMSO}-d_6$) δ /ppm 10.22 (s, 1H), 8.28 (s, 1H), 8.26 (s, 1H), 7.95 (t, $J = 7.0$ Hz, 2H), 7.44–7.24 (m, 14 H), 6.70 (s, 1H); ^{13}C NMR (75 MHz, $\text{DMSO}-d_6$) δ /ppm 153.5, 145.9, 145.7, 136.5, 132.1, 131.8, 129.8, 128.6, 128.1, 128.0, 127.7, 127.6, 127.3, 127.1, 126.7, 126.6, 126.4, 126.2, 125.6, 124.2, 122.3, 108.5, 81.6, 74.2, 54.9; IR (KBr) $\nu_{\text{max}}/\text{cm}^{-1}$ 3367 (O-H), 3051 (C-H), 3024 (C-H), 1447 (C-H); HRMS (MALDI) calculated for $\text{C}_{27}\text{H}_{19}\text{O}^+$ 359.1430, found 359.1433.

2-Methoxy-3-(diphenylhydroxymethyl)anthracene (7OMe). The reaction was carried out in a two-neck round-bottom flask (25 mL) under a N_2 atmosphere. 2-Hydroxy-3-(diphenylhydroxymethyl)anthracene (7, 18 mg, 48 μmol) was dissolved in acetone (8 mL),

and K_2CO_3 (50 mg, 362 μmol) was added. The resulting suspension was heated at reflux, resulting in a change of the color from pale yellow to yellow. MeI (50 μL , 803 μmol) was then added, and the reaction mixture was stirred for 5 h at rt (the color returns to pale yellow). The reaction mixture was then filtered, and the filtrate was evaporated on a rotary evaporator. The residue product was purified on a short column of silica gel (10 × 1 cm) using CH_2Cl_2 as eluent to give pure 2-methoxy-3-(diphenylhydroxymethyl)anthracene (7OMe, 11 mg, 31 μmol , 64% yield) in the form of a pale yellow solid. ^1H NMR (600 MHz, CDCl_3) δ /ppm 8.25 (s, 1H), 8.12 (s, 1H), 7.92 (d, $J = 8.4$ Hz, 1H), 7.86 (d, $J = 8.4$ Hz, 1H), 7.44–7.40 (m, 2H), 7.34–7.28 (m, 11H), 7.11 (s, 1H), 5.19 (s, 1H), 3.79 (s, 3H); ^{13}C NMR (150 MHz, CDCl_3) δ /ppm 155.9 (s), 146.3 (s), 136.8 (s), 132.3 (s), 131.8 (s), 130.7 (s), 130.1 (d), 128.1 (d), 128.0 (d), 127.8 (d), 127.7 (d), 127.5 (d), 127.3 (s), 127.0 (d), 125.6 (d), 124.6 (d), 123.5 (d), 105.7 (d), 82.1 (s), 55.6 (q); IR (KBr) $\nu_{\text{max}}/\text{cm}^{-1}$ 3448 (O-H), 2920 (C-H), 2851 (C-H), 1458 (C-H); HRMS (MALDI) calculated for $\text{C}_{28}\text{H}_{22}\text{O}_2^+$ 390.1614, found 390.1624.

Irradiation Experiments. Preparative Photomethanolysis. In a quartz vessel was placed a $\text{CH}_3\text{OH}-\text{H}_2\text{O}$ (4:1) solution of compound 7 (100 mL, $c \sim 4 \times 10^{-4}$ M), and it was irradiated in a Rayonet reactor using 16 lamps at 350 nm. Prior to, and during the irradiation, the solution was continuously purged with a stream of Ar and cooled by a coldfinger condenser. After 90 min of irradiation, the solvent was removed on a rotary evaporator and the residue was dried (water was removed as azeotrope with toluene). The photoproduct was purified on a column of silica gel (4 × 1 cm) using CH_2Cl_2 as eluent to obtain pure 9 (13 mg, 33 μmol , 84% yield) in the form of a pale yellow film on the walls of the flask. ^1H NMR (600 MHz, CDCl_3) δ /ppm 8.68 (s, 1H), 8.20 (s, 1H), 8.19 (s, 1H), 7.90 (d, $J = 8.4$ Hz, 1H), 7.86 (d, $J = 8.4$ Hz, 1H), 7.68 (s, 1H), 7.46–7.42 (m, 4H), 7.41–7.31 (m, 8H), 3.35 (s, 3H); ^{13}C NMR (150 MHz, CDCl_3) δ /ppm 153.9 (s), 140.6 (s), 132.6 (s), 132.4 (s), 132.1 (s), 130.5 (d), 129.0 (d), 128.1 (d), 128.0 (d), 127.9 (d), 127.5 (d), 126.9 (s), 126.7 (d), 125.5 (d), 124.2 (d), 123.0 (d), 110.1 (d), 53.1 (q); IR (KBr) $\nu_{\text{max}}/\text{cm}^{-1}$ 3421 (O-H), 3055 (C-H), 2970 (C-H), 2924 (C-H), 2953 (C-H), 1448 (C-H); HRMS (MALDI) calculated for $\text{C}_{27}\text{H}_{20}\text{O}^+$ 360.1509, found 360.1506.

Irradiation in the Presence of NaN_3 . In a quartz vessel was placed CH_3CN solution (70 mL) of compound 7 (15 mg, 40 μmol), and a solution of NaN_3 (1 g, 15 mmol) in water (30 mL) was added. Upon addition of NaN_3 , the solution changed color to yellow, probably due to deprotonation of the anthrol OH (caused by hydrolysis of the azide). The solution was irradiated in a reactor using 12 lamps at 350 nm for 2 h. Prior to, and during the irradiation, the solution was continuously purged with a stream of Ar and cooled using a coldfinger condenser. After the irradiation, the reaction mixture was poured on water (150 mL) and extracted with diethyl ether (3 × 20 mL). The organic extracts were combined and washed with water (2 × 100 mL). The organic phase was separated and dried over anhydrous MgSO_4 and filtered, and the solvent was removed on a rotary evaporator. The crude product was chromatographed on a short column of silica gel (10 × 1 cm) using CH_2Cl_2 as an eluent to obtain pure product 10 (6 mg, 15 μmol , 38% yield) in the form of a thin yellowish film on the walls of the flask. ^1H NMR (600 MHz, CDCl_3) δ /ppm 8.23 (s, 1H), 8.18 (s, 1H), 7.92 (d, $J = 8.4$ Hz, 1H), 7.86 (d, $J = 8.4$ Hz, 1H), 7.44–7.41 (m, 8H), 7.39 (s, 1H), 7.30 (m, 4H), 6.92 (s, 1H); ^{13}C NMR (150 MHz, CDCl_3) δ /ppm 152.4 (s), 140.9 (s), 132.54 (s), 132.46 (s), 131.4 (s), 130.9 (d), 130.4 (s), 128.6 (d), 128.4 (d), 128.3 (d), 128.2 (d), 128.1 (d), 127.6 (d), 127.1 (d), 126.8 (s), 125.6 (d), 124.5 (d), 123.2 (d), 111.3 (d), 29.6 (s); IR (KBr) $\nu_{\text{max}}/\text{cm}^{-1}$ 3421 (O-H), 3057 (C-H), 2924 (C-H), 2853 (C-H), 2104 ($\text{N}\equiv\text{N}$); HRMS (MALDI) calculated for $\text{C}_{27}\text{H}_{20}\text{O}^+$ 360.1509, found 360.1523.

Irradiation in the Presence of 2,2,2-Trifluoroethanol (TFE). In a quartz vessel was placed a CH_3CN solution (90 mL) of compound 7 (13 mg, 35 μmol), and 2,2,2-trifluoroethanol (10 mL) was added. The solution was irradiated in a reactor using 12 lamps at 350 nm for 30 min. Prior to, and during the irradiation, the solution was continuously purged with a stream of Ar and cooled using a coldfinger condenser. After the irradiation, the solvent was evaporated on a rotary

evaporator. The crude product was chromatographed on a short column of silica gel (10 × 1 cm) using CH₂Cl₂ as an eluent to obtain the pure product **11** (6 mg, 13 μmol, 37% yield) in the form of a thin yellowish film on the walls of the flask. ¹H NMR (600 MHz, CDCl₃) δ/ppm 8.22 (2s, 2H), 7.92 (d, *J* = 8.8 Hz, 1H), 7.87 (d, *J* = 8.8 Hz, 1H), 7.72 (s, 1H), 7.49–7.45 (m, 4H), 7.43–7.35 (m, 9H), 3.77 (q, ³*J*_{H,F} = 8.1 Hz, 2H); ¹³C NMR (150 MHz, CDCl₃) δ/ppm 152.9 (s), 139.7 (s), 132.64 (s), 132.58 (s), 132.4 (s), 130.9 (d), 130.4 (s), 128.6 (d), 128.5 (d), 128.3 (d), 128.1 (d), 127.6 (d), 127.0 (d), 126.9 (s), 125.8 (d), 125.5 (q, ¹*J*_{C,F} = 251 Hz), 124.5 (d), 123.2 (d), 111.0 (d), 62.7 (q, ³*J*_{C,H} = 34 Hz), 29.6 (s); IR (KBr) ν_{max}/cm⁻¹ 3435 (O–H), 3059 (C–H), 2924 (C–H), 2953 (C–H), 1281 (C–F), 1165 (C–F); HRMS (MALDI) calculated for C₂₇H₂₀O⁺ 360.1509, found 360.1504.

Quantum Yield of the Photomethanolysis Reaction. Quantum yield of the photomethanolysis reaction was determined by use of three actinometers simultaneously: valerophenone,²⁴ ferrioxalate,²⁵ and KI/KIO₃.³² A solution of ferrioxalate actinometer was handled in the dark. The measurement was performed in five quartz cells with the same dimensions (square, for UV–vis measurement, ca. 3 mL), which were, during the irradiations, wrapped in black paper, except from the front side to ensure the controlled absorption of the light from one side only (no absorption of the radiation reflected from the walls of the reactor). The solution of compound **7** in CH₃OH–H₂O (4:1) and the solution of valerophenone in CH₃CN–H₂O (4:1) were freshly prepared, and their concentrations were adjusted to have absorbances of 0.4–0.8 at 254 nm. After adjustment of the concentrations and measurement of the corresponding UV–vis spectra, 2.5 mL of the solution was transferred to the quartz cell and the solutions were purged with a stream of N₂ (20 min each), and then sealed with a cap. A freshly prepared solution of potassium trioxalatoferate(III) (0.012 M K₃[Fe(C₂O₄)₃] × 3H₂O in 0.05 M H₂SO₄) (2.5 mL) and the solution containing potassium iodate (0.1 M) and potassium iodide (0.6 M) in borate buffer (pH = 9.25) (2.5 mL) were placed in the third and the fourth quartz cells, respectively. Potassium trioxalatoferate(III) (2.5 mL) was placed in the fifth cell, which was not irradiated (blank sample). Before the irradiation, A₃₅₂ for the solution of KI/KIO₃ was measured. The cells were placed in a holder, which ensured equal distance of all samples from the lamp, and irradiated at the same time in the reactor with 1 lamp at 254 nm for 30 s. Before and after the irradiation, the samples were taken from the cells by use of a syringe and analyzed by HPLC to determine conversion of **7** to **9** and valerophenone to acetophenone. The conversion did not exceed 30% to avoid change of the absorbance, or filtering of the light by the product. A₃₅₂ of KI/KIO₃ actinometer solution was measured to determine the concentration of I₃⁻ using ε₃₅₂ = 27 600 M⁻¹ cm⁻¹.³² To both solutions of ferrioxalate actinometer (irradiated and blank) was added a solution of phenanthroline (0.5 mL, 0.1% phenanthroline in buffer containing 1.65 M NaOAc and 0.5 M H₂SO₄), and A₅₁₀ was measured. The concentration of Fe^{II} was determined using ε₅₁₀ = 11 100 M⁻¹ cm⁻¹.²⁵ From the conversion (valerophenone) and concentration of the photoproducts (in ferrioxalate and KI/KIO₃), irradiance was calculated. The similar values were obtained for all three actinometers. These values and the value of conversion **7** → **9** were used to calculate the quantum yield of photomethanolysis for compound **7**. The mean value of three measurements was reported. All equations for the calculation of quantum yields are given in the Supporting Information.

Steady-State and Time-Resolved Fluorescence Measurements.

The steady-state measurements were performed using a luminescence spectrometer. The samples were dissolved in CH₃CN or CH₃CN–H₂O (1:1), and the concentrations were adjusted to have absorbances at the excitation wavelength (330, 350, or 370 nm) < 0.1. Solutions were purged with nitrogen for 30 min prior to analysis. The measurements were performed at 20 °C. Fluorescence quantum yields were determined by comparison of the integral of the emission bands with the one of quinine sulfate in 0.05 M aqueous H₂SO₄ (Φ_F = 0.53). The measurements were performed in triplicate, and the mean value was reported. Typically, three absorption traces were recorded (and averaged) and three fluorescence emission traces, exciting at three different wavelengths. Three quantum yields were calculated, and the mean value was reported.

Fluorescence decays were obtained on an instrument equipped with a light-emitting diode (excitation wavelength = 375 nm), using a time-correlated single-photon counting technique in 1023 channels. Histograms of the instrument response functions (using LUDOX scatterer), and sample decays, were recorded at 410, 420, 450, and 550 nm until they reached 2 × 10³ counts in the peak channel. The half-width of the instrument response function was ≈ 0.2 ns. The time increment per channel was 0.02441 ns. Obtained histograms were fitted as sums of exponential using a Gaussian-weighted nonlinear least-squares fitting based on Marquardt–Levenberg minimization implemented in the software package of the instrument. The fitting parameters (decay times and pre-exponential factors) were determined by minimizing the global reduced chi-squared, χ². An additional graphical method was used to judge the quality of the fit that included plots of surfaces (“carpets”) of the weighted residuals versus channel number.

Determination of pK_a and pK_a* for 2-Anthrol (8**).** UV–vis Titration. A stock solution of the compound **8** was prepared by dissolving **8** (0.50 mg) in CH₃CN (500 μL). A 195 μL aliquot of the stock solution was diluted to 200 mL with CH₃CN–H₂O (1:9) to adjust the concentration of the compound to 5.0 × 10⁻⁶ M (for titration I). For titration II, **8** (7.93 mg) was dissolved in 200 mL of CH₃CN/H₂O (2:8). A 150.0 mL portion of each solution was titrated with a diluted solution of NaOH (until pH 12.7 was reached). The pH was measured by a pH meter, and UV–vis spectra were recorded on an instrument. The measurement was performed at 25 °C. The resulting UV–vis spectra were processed by multivariate nonlinear regression analysis using the Specfit program.

Fluorescence Titration. A stock solution of the compound **8** was prepared by dissolving **8** (1 mg) in CH₃CN (1000 μL). A 855 μL aliquot of the stock solution was diluted to 200 mL with CH₃CN–H₂O (1:9) to adjust the concentration of the compound to 2.2 × 10⁻⁵ M. A 150.0 mL portion of the solution was basified with a diluted solution of NaOH (until pH 12.3 was reached) and titrated with a diluted solution of H₂SO₄ (until pH 0.5 was reached). The pH was measured by a pH meter, and fluorescence spectra were recorded on an instrument (slits 2 × 2.5 nm). The measurement was performed at 25 °C. The resulting fluorescence spectra were processed by multivariate nonlinear regression analysis using the Specfit program.

Laser Flash Photolysis (LFP). All LFP studies were conducted at the University of Victoria LFP facility employing a YAG laser, with a pulse width of 10 ns and an excitation wavelength of 355 nm. Static cells (0.7 cm) were used, and solutions were purged with nitrogen or oxygen for 20 min prior to measurements. Absorbances at 355 nm were ~0.4.

Antiproliferative Investigation. The experiments were carried out on three human carcinoma cell lines, HCT 116, MCF-7, and H 460. Cells were cultured as monolayers and maintained in Dulbecco’s modified Eagle medium (DMEM) supplemented with 10% fetal bovine serum (FBS), 2 mM L-glutamine, 100 U/mL penicillin, and 100 μg/mL streptomycin in a humidified atmosphere with 5% CO₂ at 37 °C.

The cells were inoculated in parallel on two 96-well microtiter plates on day 0, at 1.5 × 10⁴ cells/mL. Test agents were added in 10-fold dilutions (10⁻⁸ to 10⁻⁴ M) on the next day and incubated for a further 72 h. Working dilutions were freshly prepared on the day of testing. One of the plates was left in the dark, whereas the other was irradiated in a reactor (6 lamps 350 or 420 nm, 5 min) for 4, 24, and 48 h after the addition of the compounds. After 72 h of incubation, the cell growth rate was evaluated by performing the MTT assay³³ (for the irradiated and nonirradiated cells), which detects dehydrogenase activity in viable cells. The absorbance (*A*) was measured on a microplate reader at 570 nm. The absorbance is directly proportional to the number of living, metabolically active cells. The percentage of growth (PG) of the cell lines was calculated according to one or the other of the following two expressions: If (mean *A*_{test} – mean *A*_{tzero}) ≥ 0, then PG = 100 × (mean *A*_{test} – mean *A*_{tzero}) / (mean *A*_{ctrl} – mean *A*_{tzero}). If (mean *A*_{test} – mean *A*_{tzero}) < 0, then PG = 100 × (mean *A*_{test} – mean *A*_{tzero}) / *A*_{tzero} where the mean *A*_{tzero} is the average of absorbance measurements before exposure of cells to the test compound, the mean

A_{test} is the average of absorbance measurements after the desired period of time, and the mean A_{ctrl} is the average of absorbance measurements after the desired period of time with no exposure of cells to the test compound. In the experiments where the cells were irradiated, A_{ctrl} represents irradiated control cells. After irradiation at 350 nm, 25% growth inhibition compared to A_{ctrl} without irradiation was observed, whereas, after the irradiation at 420 nm, no significant growth inhibition was observed.

The results are expressed as IC_{50} , which is the concentration necessary for 50% of inhibition. The IC_{50} values are calculated from concentration–response curves using linear regression analysis by fitting the test concentrations that give PG values above and below the reference value (i.e., 50%). Each test was performed in quadruplicate in at least two individual experiments.

■ ASSOCIATED CONTENT

■ Supporting Information

The contents of the Supporting Information include copies of the ^1H and ^{13}C NMR spectra and UV–vis, fluorescence, and LFP data. This material is available free of charge via the Internet at <http://pubs.acs.org>.

■ AUTHOR INFORMATION

Corresponding Author

*Fax: + 385 1 4680 195. Tel: +385 1 4561 141. E-mail: nbasaric@irb.hr.

Notes

The authors declare no competing financial interest.

■ ACKNOWLEDGMENTS

This work was supported by the Croatia Foundation for Science (HRZZ grant no. 02.05/25), the Ministry of Science Education and Sports of the Republic of Croatia (grant No. 098-0982933-2911), the Natural Sciences and Engineering Research Council (NSERC) of Canada, and the University of Victoria.

■ REFERENCES

- (1) Rokita, S. E., Ed. *Quinone Methides*; Wiley: Hoboken, NJ, 2009.
- (2) (a) McCracken, P. G.; Bolton, J. L.; Thatcher, G. R. J. *J. Org. Chem.* **1997**, *62*, 1820–1825. (b) Modica, E.; Zanaletti, R.; Freccero, M.; Mella, M. *J. Org. Chem.* **2001**, *66*, 41–52.
- (3) Bolton, J. L.; Turnipseed, S. B.; Thompson, J. A. *Chem.-Biol. Interact.* **1997**, *107*, 185–200.
- (4) (a) McDonald, I. A.; Nyce, P. L.; Jung, M. J.; Sabol, J. S. *Tetrahedron Lett.* **1991**, *32*, 887–890. (b) Wang, Q.; Myers, J. K.; Cohen, J. D.; Widlanski, T. S. *J. Am. Chem. Soc.* **1995**, *117*, 11049–11054. (c) Storwell, J. K.; Widlanski, T. S.; Kutaleladze, T. G.; Raines, R. T. *J. Org. Chem.* **1995**, *60*, 6930–6936. (d) Cabaret, D.; Adediran, S. A.; Gonzalez, M. J. G.; Pratt, R. F.; Wakselman, M. *J. Org. Chem.* **1999**, *64*, 713–720.
- (5) (a) Rokita, S. E.; Yang, J.; Pande, P.; Greenberg, W. A. *J. Org. Chem.* **1997**, *62*, 3010–3012. (b) Veldhuyzen, W. F.; Shallop, A. J.; Jones, R. A.; Rokita, S. E. *J. Am. Chem. Soc.* **2001**, *123*, 11126–11132.
- (6) (a) Pande, P.; Shearer, J.; Yang, J.; Greenberg, W. A.; Rokita, S. E. *J. Am. Chem. Soc.* **1999**, *121*, 6773–6779. (b) Wang, P.; Liu, R.; Wu, X.; Ma, H.; Cao, X.; Zhou, P.; Zhang, J.; Weng, X.; Zhang, X. L.; Zhou, X.; Weng, L. *J. Am. Chem. Soc.* **2003**, *125*, 1116–1117. (c) Richter, S. N.; Maggi, S.; Colloredo Mels, S.; Palumbo, M.; Freccero, M. *J. Am. Chem. Soc.* **2004**, *126*, 13973–13979. (d) Verga, D.; Richter, S. N.; Palumbo, M.; Gandolfi, R.; Freccero, M. *Org. Biomol. Chem.* **2007**, *5*, 233–235.
- (7) (a) Wolkenberg, S. E.; Boger, D. L. *Chem. Rev.* **2002**, *102*, 2477–2495. (b) Wang, P.; Song, Y.; Zhang, L.; He, H.; Zhou, X. *Curr. Med. Chem.* **2005**, *12*, 2893–2913.
- (8) (a) Li, V. S.; Kohn, H. *J. Am. Chem. Soc.* **1991**, *113*, 275–283. (b) Han, I.; Russell, D. J.; Kohn, H. *J. Org. Chem.* **1992**, *57*, 1799–1807. (c) Tomasz, M.; Das, A.; Tang, K. S.; Ford, M. G. J.; Minnock, A.; Musser, S. M.; Waring, M. J. *J. Am. Chem. Soc.* **1998**, *120*, 11581–11593.
- (9) (a) Abdella, B. R. J.; Fisher, J. *Environ. Health Perspect.* **1985**, *64*, 4–18. (b) Engholm, M.; Koch, T. H. *J. Am. Chem. Soc.* **1989**, *111*, 8291–8293. (c) Angle, S. R.; Yang, W. *J. Am. Chem. Soc.* **1990**, *112*, 4524–4528. (d) Gaudiano, G.; Frigerio, M.; Bravo, P.; Koch, T. H. *J. Am. Chem. Soc.* **1990**, *112*, 6704–6709. (e) Gaudiano, G.; Koch, T. H. *Chem. Res. Toxicol.* **1991**, *4*, 2–16. (f) Angle, S. R.; Yang, W. *J. Org. Chem.* **1992**, *57*, 1092–1097. (g) Angle, S. R.; Rainer, J. D.; Woytowicz, C. *J. Org. Chem.* **1997**, *62*, 5884–5892.
- (10) Koch, T. H.; Barthel, B. L.; Kalet, B. T.; Rudnicki, D. L.; Post, G. C.; Burkhart, D. *J. Top. Curr. Chem.* **2008**, *283*, 141–170.
- (11) Diao, L.; Yang, C.; Wan, P. *J. Am. Chem. Soc.* **1995**, *117*, 5369–5370.
- (12) Chiang, Y.; Kresge, A. J.; Zhu, Y. *J. Am. Chem. Soc.* **2002**, *124*, 6349–6356.
- (13) Nakatani, K.; Higashida, N.; Saito, I. *Tetrahedron Lett.* **1997**, *38*, 5005–5008.
- (14) (a) Brousmiche, D.; Xu, M.; Lukeman, M.; Wan, P. *J. Am. Chem. Soc.* **2003**, *125*, 12961–12970. (b) Xu, M.; Lukeman, M.; Wan, P. *Photochem. Photobiol.* **2006**, *82*, 50–56.
- (15) (a) Lukeman, M.; Veale, D.; Wan, P.; Munasinghe, V. R.; Corrie, J. E. T. *Can. J. Chem.* **2004**, *82*, 240–253. (b) Verga, D.; Nadai, M.; Doria, F.; Percivalle, C.; Di Antonio, M.; Palumbo, M.; Richter, S. N.; Freccero, M. *J. Am. Chem. Soc.* **2010**, *132*, 14625–14637.
- (16) Arumugam, S.; Popik, V. V. *J. Am. Chem. Soc.* **2009**, *131*, 11892–11899.
- (17) Kulikov, A.; Arumugam, S.; Popik, V. V. *J. Org. Chem.* **2008**, *73*, 7611–7615.
- (18) (a) Arumugam, S.; Popik, V. V. *J. Am. Chem. Soc.* **2011**, *133*, 15730–15736. (b) Arumugam, S.; Popik, V. V. *J. Am. Chem. Soc.* **2012**, *134*, 8408–8411.
- (19) (a) Basarić, N.; Žabčić, I.; Mlinarić-Majerski, K.; Wan, P. *J. Org. Chem.* **2010**, *75*, 102–116. (b) Basarić, N.; Cindro, N.; Bobinac, D.; Mlinarić-Majerski, K.; Uzelac, L.; Kralj, M.; Wan, P. *Photochem. Photobiol. Sci.* **2011**, *10*, 1910–1925. (c) Basarić, N.; Cindro, N.; Bobinac, D.; Mlinarić-Majerski, K.; Uzelac, L.; Kralj, M.; Wan, P. *Photochem. Photobiol. Sci.* **2012**, *11*, 381–396. (d) Veljković, J.; Uzelac, L.; Molčanov, K.; Mlinarić-Majerski, K.; Kralj, M.; Wan, P.; Basarić, N. *J. Org. Chem.* **2012**, *77*, 4596–4610.
- (20) Doria, F.; Richter, S. N.; Nadai, M.; Colloredo-Mels, S.; Mella, M.; Palumbo, M.; Freccero, M. *J. Med. Chem.* **2007**, *50*, 6570–6579.
- (21) (a) Doria, F.; Nadai, M.; Folini, M.; Scalabrin, M.; Germani, L.; Sattin, G.; Mella, M.; Palumbo, M.; Zaffaroni, N.; Fabris, D.; Freccero, M.; Richter, S. N. *Chemistry* **2013**, *19*, 78–81. (b) Doria, F.; Nadai, M.; Folini, M.; Di Antonio, M.; Germani, L.; Percivalle, C.; Sissi, C.; Zaffaroni, N.; Alcaro, S.; Artese, A.; Richter, S. N.; Freccero, M. *Org. Biomol. Chem.* **2012**, *10*, 2798–2806. (c) Nadai, M.; Doria, F.; Di Antonio, M.; Sattin, G.; Germani, L.; Percivalle, C.; Palumbo, M.; Richter, S. N.; Freccero, M. *Biochimie* **2011**, *93*, 1328–1340.
- (22) Rochlin, E.; Rappoport, Z. *J. Org. Chem.* **2003**, *68*, 216–226.
- (23) Albrecht, M.; Bohne, C.; Grazhnan, A.; Ihmels, H.; Pace, T. C. S.; Schnurpfeil, A.; Waidelich, M.; Yihwa, C. *J. Phys. Chem. A* **2007**, *111*, 1036–1044.
- (24) Montalti, M.; Credi, A.; Prodi, L.; Gandolfi, M. T. *Handbook of Photochemistry*; CRC Taylor and Francis: Boca Raton, FL, 2006.
- (25) Solntsev, K. M.; Huppert, D.; Agmon, N.; Tolbert, L. M. *J. Phys. Chem. A* **2000**, *104*, 4658–4669.
- (26) Kuhn, H. J.; Braslavsky, S. E.; Schmidt, R. *Pure Appl. Chem.* **2004**, *76*, 2105–2146.
- (27) (a) Dixon, W. T.; Murphy, D. J. *Chem. Soc., Faraday Trans. 2* **1976**, *72*, 1221–1230. (b) Brodwell, F. G.; Cheng, J.-P. *J. Am. Chem. Soc.* **1991**, *113*, 1736–1743. (c) Gadosy, T. A.; Shukla, D.; Johnston, L. J. *J. Phys. Chem. A* **1999**, *103*, 8834–8839.
- (28) (a) Kleinman, M. H.; Flory, J. H.; Tomalia, D. A.; Turro, N. J. *J. Phys. Chem. B* **2000**, *104*, 11472–11479. (b) Pretali, L.; Doria, F.; Verga, D.; Profumo, A.; Freccero, M. *J. Org. Chem.* **2009**, *74*, 1034–1041.

(29) (a) McClelland, R. A.; Chan, C.; Cozens, F. L.; Modro, A.; Steenken, S. *Angew. Chem., Int. Ed.* **1991**, *30*, 1337–1339. (b) Cozens, F. L.; Kanagasabapathy, V. M.; McClelland, R. A.; Steenken, S. *Can. J. Chem.* **1999**, *77*, 2069–2082.

(30) (a) McClelland, R. A.; Banait, N.; Steenken, S. *J. Am. Chem. Soc.* **1986**, *108*, 7023–7027. (b) McClelland, R. A.; Kanagasabapathy, V. M.; Banait, N. S.; Steenken, S. *J. Am. Chem. Soc.* **1989**, *111*, 3966–3972.

(31) Saha, K.; Lajis, N. H.; Abas, F.; Najj, N. A.; Hamzah, A. S.; Shaari, K. *Aust. J. Chem.* **2008**, *61*, 821–825.

(32) (a) Goldstein, S.; Rabani, J. *J. Photochem. Photobiol.* **2008**, *193*, 50–55. (b) Rahn, R. O. *Photochem. Photobiol.* **1997**, *66*, 450–455.

(33) (a) Mossman, T. *J. Immunol. Meth.* **1983**, *65*, 5563. (b) Boyd, M. R.; Kenneth, D. P. *Drug. Dev. Res.* **1995**, *34*, 91–109.